Diffusion in Heterogeneous Media: Application to Immobilized Cell Systems

Mark R. Riley, Fernando J. Muzzio, and Helen M. Buettner
Dept. of Chemical and Biochemical Engineering, Rutgers University, Piscataway, NJ 08855

Sebastian C. Reyes
Corporate Research Lab., Exxon Research and Engineering Co., Annandale, NJ 08801

Transport of small molecules in heterogeneous materials can be an important factor in many engineering and biological applications. This study focuses on the diffusion of cellular nutrients in an immobilized cell system. A Monte Carlo simulation technique is used to describe the diffusion of small molecules in a variety of simulated cellular structures. Diffusivity predictions are in close agreement with experimental values as well as with theoretical bounds reported in the literature. It is revealed that effective diffusivities are highly dependent on the diffusivities of the species in the various phases and on the volume fraction of cells. The spatial arrangement of the cells, however, has no apparent effect on the predicted diffusivity for the range of conditions investigated.

Introduction

Composite materials consisting of one or more dispersed phases distributed in a single continuous phase arise in a wide variety of engineering and biological systems. Examples include packed beds, polymer blends, ceramic precursors, biofilms, soil, and many forms of biological tissue. The transport of substances in these materials often critically affects the performance of such systems. Transport rates generally depend on diffusive, convective, and reactive mechanisms as well as on the structural characteristics of the material. For example, the amount of long-term deterioration of marble structures by acid rain is controlled by the rate of diffusion and reaction of SO_x in the marble. Diffusion can also be the rate-limiting factor in many biological processes, such as the supply of nutrients received by cells in tissues, the transport of substances through the intestinal wall, and the rate of growth of nutrient-limited biofilms.

This article focuses on a subset of composite materials in which transport arises exclusively from molecular diffusion; we assume that solutions are dilute and that bulk flow is negligible. Diffusion is driven by random molecular motion and the overall flux is well described by a volume-averaged version of Fick's law:

$$F_i = -D_{\text{eff}} \nabla C_i, \tag{1}$$

where the vector F_i is the flux of species i at some position in space, ∇C_i is the gradient of the volume-averaged concentration of i, and D_{eff} is the effective diffusivity that includes contributions to flux through all conductive phases. The ability to accurately measure or predict D_{eff} over a wide range of conditions is critical for describing the behavior of the multiphase system. However, accurate measurement of D_{eff} is difficult due to a number of factors: (1) D_{eff} depends nontrivially on the species diffusivities and volume fractions of all the contributing phases (and for systems such as soil, the number of phases can be large and species diffusivities unknown); (2) D_{eff} can depend strongly on structural characteristics, that is, the pore size distribution and the particle size distribution; moreover, in some materials, the structure evolves with time, as in heterogeneous catalysts undergoing sintering and in immobilized cell systems with actively proliferating cells; and (3) experimental D_{eff} measurements are often complicated by the presence of reactions. This latter difficulty can sometimes be circumvented if the reaction kinetics are known accurately, but then the opposite problem arises, because kinetic measurements can be affected by diffusional limitations.

The most widely used approach for predicting D_{eff} follows from Maxwell's equation (1954), which was originally derived to describe electrical conduction in a heterogeneous material. In the context of diffusion, Maxwell's model can be ex-

Correspondence concerning this article should be addressed to F. J. Muzzio.

pressed as:

$$\frac{D_{\text{eff}}}{D_0} = \frac{2D_0 + D_c - 2\phi(D_0 - D_c)}{2D_0 + D_c + \phi(D_0 - D_c)}, \qquad (2)$$

where D_0 is the diffusivity of a given species through the continuous phase, D_c is the diffusivity through the dispersed phase, and ϕ is the volume fraction of the dispersed phase. This model has been frequently applied to predict D_{eff} in numerous heterogeneous materials [for a review on diffusion in biological systems, see Westrin and Axelsson (1991)]. The derivation of Eq. 2 assumes a fairly simplistic type of structure: the dispersed phase is composed of monosized, nonoverlapping, spherical inclusions, randomly placed throughout the continuous phase, and therefore, this model is accurate only at very low inclusion fractions.

Statistical and geometrical approaches have also been useful for estimating diffusivities in heterogeneous systems. Hashin and Shtrikman (1962) used variational principles to generate diffusivity bounds for macroscopically homogeneous materials based on the volume fractions of each phase and the species diffusivity in each phase. Wakao and Smith (1962, 1964) developed a phenomenological "random pore" model, to predict D_{eff} in a bimodal pore structure of a porous catalyst.

These approaches provide a good basis for understanding the functional dependence of diffusivities in terms of volume fractions, but lack the detail and specificity to describe the actual morphological characteristics observed in real systems. Typically, the dispersed phase components are distributed neither in a regular array nor in completely random positions; an intermediate degree of order is often observed. Monte Carlo simulations provide an efficient alternative for studying such systems and have been used to investigate diffusion of gas molecules in porous systems with impenetrable structural backbones. The backbone was represented as a network of nonconductive inclusions, so that diffusion occurs only in the continuous phase (Evans et al., 1980; Reyes and Iglesia, 1991a,b; Kim and Torquato, 1992a,b).

Biological systems can be significantly more complex than porous solids. Typically, all the phases allow a finite rate of solute transport (the backbone is no longer impenetrable). Situations in which all phases allow some amount of solute diffusion have been the focus of just a handful of studies (Chiew and Glandt, 1983; Chiew, 1990; Kim and Torquato, 1990, 1991; Tobochnik et al., 1990; Cukier et al., 1990). These studies considered inclusions that were more conductive than the continuous phase, and cannot reliably be applied to describe diffusion through populations of immobilized cells in which the inclusions (the cells) are less conductive than the support (Westrin and Axelsson, 1991). Our study focuses on systems where the molecular species of interest diffuses through the continuous phase with diffusivity D_0, and through the inclusion phase with diffusivity D_c, such that $D_0 > D_c$. Investigation of this case is important because the transport of nutrients and cellular products to and from immobilized cells is a limiting factor in the productivity of many biological systems.

This article is organized as follows: Experimentally measured diffusivities in immobilized cell systems are reviewed in the following section. The third section describes simulation procedures to represent populations of immobilized cells and to determine effective diffusivities in such structures. The procedure is used to represent a variety of cell systems by manipulating D_0, D_c, and the spatial distribution of cells. Diffusivity results in two- and three-dimensional systems are presented and discussed in the fourth section. Finally, conclusions and future work are discussed in the last section.

Diffusion in Immobilized Cell Systems

Viable, metabolically active cells retained within a support are the basis of a wide variety of natural and man-made biological systems, including tissue, biofilms, tumor microspheres, cell-based artificial organs, and encapsulated cell bioreactors. Encapsulation of cells for use in a bioreactor has several advantages over conventional suspension culture methods. Immobilization allows the attainment of larger cell densities inside a bioreactor, protects fragile mammalian cells from shear forces, and simplifies product purification. Immobilization also can increase the productivity of some cell types (Lee and Palsson, 1990, 1993). These advantages have contributed to the development of several engineering applications in which viable cells encapsulated in gelatinous beads (see Figure 1) are cultivated in bioreactors for the manufacture of valuable biological products such as antibodies, vaccines, interferons, and growth factors (Karel et al., 1985).

The behavior of immobilized cell systems is governed by the interplay of nutrient and product diffusion, cell metabolism, and cell proliferation. Diffusion plays an important role because cells retained inside a gelatinous bead do not receive nutrients by convective mechanisms. As the cells proliferate, the total nutrient consumption increases as do the diffusive limitations, leading to a demand that cannot be met by the prevailing diffusion rates. This leads to undesired concentration gradients in the nutrient levels (see Figure 1) and can confine the cellular metabolic activity to the vicinity of the interface between the growth media and the cell-containing support (Lazar, 1991; Franko and Sutherland, 1979; Freyer and Sutherland, 1981). For example, Karel and Robertson (1989) observed that active cell growth of *Pseudomonas putida* in microporous hollow fibers occurred in a region less than 25 μm in depth from the oxygen supply. The lowered nutrient levels can also reduce the cellular production rates below their theoretical maximum levels. This is analogous to effectiveness factors less than unity that commonly arise in heterogeneous catalysts subject to diffusional limitations.

The effective diffusivity of a metabolite in immobilized cell systems depends on its diffusivity in both the support material and the cells. The diffusivity of a solute in a gelatinous support can be readily measured using cell-free systems. Small molecular weight solutes in dilute (1–4 w/v %, 10–40 mg/mL) gels of agarose, alginate, or κ-carrageenan diffuse with rates similar to those in water. For example, glucose exhibits diffusivities in the range $D = 5.0\text{–}6.8 \times 10^{-6}$ cm^2/s; corresponding values for oxygen are in the range $D = 2.0\text{–}2.5 \times 10^{-5}$ cm^2/s (Tanaka et al., 1984; Martinsen et al., 1989; Scott et al., 1989; Sun et al., 1989; and Boyer and Hsu, 1992). Experimental studies report conflicting trends in the effective diffusivity due to the presence of cells. Kurosawa and coworkers (1989) and

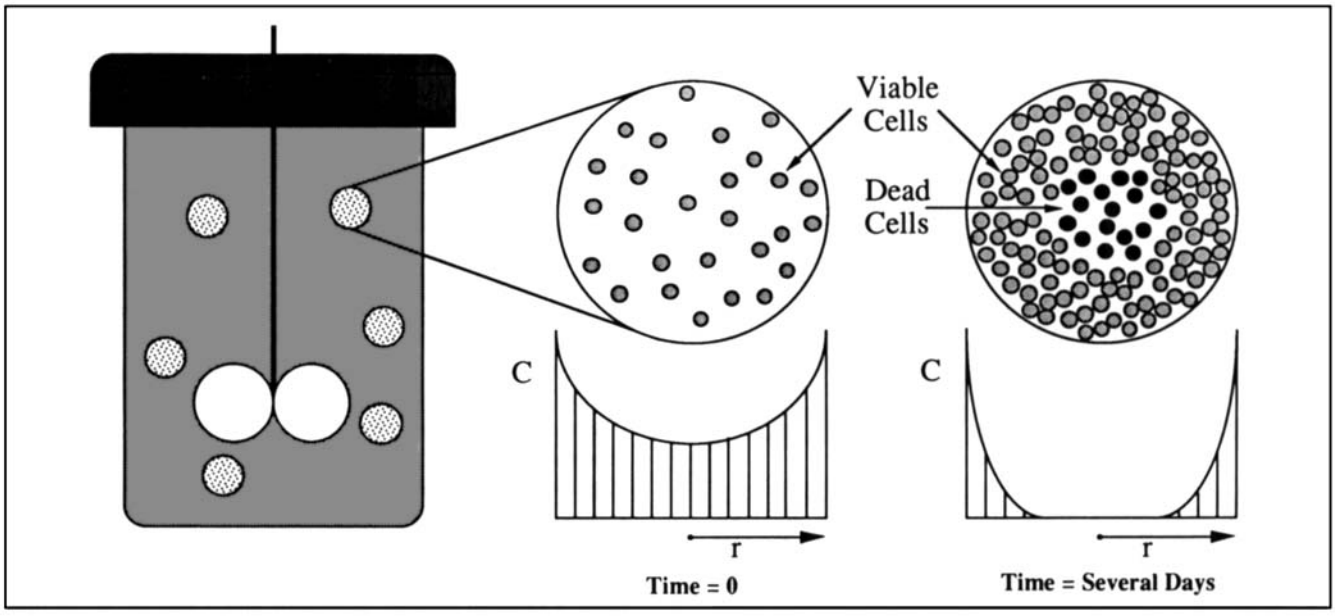

Figure 1. Stirred tank encapsulated cell bioreactor.

Blowup shows the cross section of an individual biocatalyst bead containing immobilized cells immediately after encapsulation (center) and after several days of cell growth (right). Initially, the cells are sparsely distributed throughout the support, and diffusional limitations produce only a mild decrease in nutrient levels toward the center of the bead. At later stages, increased cell density considerably reduces substrate concentration available to cells deep inside the bead.

Hannoun and Stephanopoulos (1986) reported that diffusivities of oxygen and glucose, respectively, were unaffected by the presence of cells. However, there are numerous reports in the literature that a species diffusivity is highly dependent on the cell density (Sun et al., 1989; Pu and Yang, 1988; Libicki et al., 1988; Luby-Phelps et al., 1987; and Korgel et al., 1992). For example, the effective diffusivity of glucose in tumor masses has been found to be in the range of $(0.25-0.50)D_0$, where D_0 is the diffusivity of glucose in water (Kawashiro et al., 1975). Karel and coworkers (1985) and Westrin and Axelsson (1991) published reviews on the relative diffusivity of several solutes in various cell masses and reported that the effective diffusivity generally decreases with increasing cell fraction regardless of cell type or diffusing species with values in the range of $0.01D_0 \leq D_{\text{eff}} \leq 1.1D_0$.

There are several possible explanations for the aforementioned discrepancies. Accurate quantification of diffusion in biological systems is quite complicated. The mathematical relations used to calculate the effective diffusivity from experimental data are very sensitive to small errors in evaluation of the species concentration (Itamunoala, 1988). In some cases, the diffusion coefficients may have a concentration dependence. Obviously, the molecules of greatest interest are cellular nutrients or cellular products that are consumed or produced by the cells, thus changing their concentration and complicating evaluation of diffusive properties. Several approaches have been used to attempt to remove the effect of species reactivity in diffusion experiments, but such techniques often introduce additional complications. A simulation approach permits the detailed evaluation of the effects of the cell fraction and diffusivity ratio on the overall diffusive behavior. In this study, it is assumed that the species of interest (a) diffuses through the cells with a constant diffusivity D_c, (b) diffuses through the support with a constant diffusivity D_0, (c) encounters negligible resistance due to the cell membrane, (d) does not react in either phase, and (e) the diffusion time scale, $t_d = L^2/D_{\text{eff}}$ is much shorter than the cell doubling time (where L is the macroscopic dimension of the system). These simplifications provide a well-defined starting point for our theoretical study, which predicts reasonably well the transport properties of biological systems.

Algorithms

The Monte Carlo algorithm used here is similar to those used to study transport in porous solids with impenetrable backbones (Evans et al., 1980; Abbasi et al., 1983; Nakano and Evans, 1983; Akanni and Evans, 1987; Zheng and Chiew, 1989; Reyes and Iglesia, 1991a,b; Torquato and Avellaneda, 1991). However, the method has been modified to account for tracer diffusion through both phases in a variety of structural systems. The effects of three factors on the calculated effective diffusivity (D_{eff}) are investigated: volume fraction of inclusions (cells) ϕ; placement of the cells; and the diffusivity ratio, D_0/D_c. Direct calculation of D_c can be difficult and values depend on the diffusing species and on the cell type. Experimental reports indicate values throughout the range $0 < D_c < D_0$, but the most frequently reported estimate is about 20–30% of D_0 (Westrin and Axelsson, 1991). For example, Kao and coworkers (1993) measured the diffusivity of a small fluorescent probe in the cell cytoplasm, determining D_0/D_c to be 3.70 ± 0.14 at 23°C. Therefore, we have investigated situations where $D_0/D_c = 2$, 3, 4, 5, and ∞.

Structure simulation

The simulated structure is constructed based on rules that

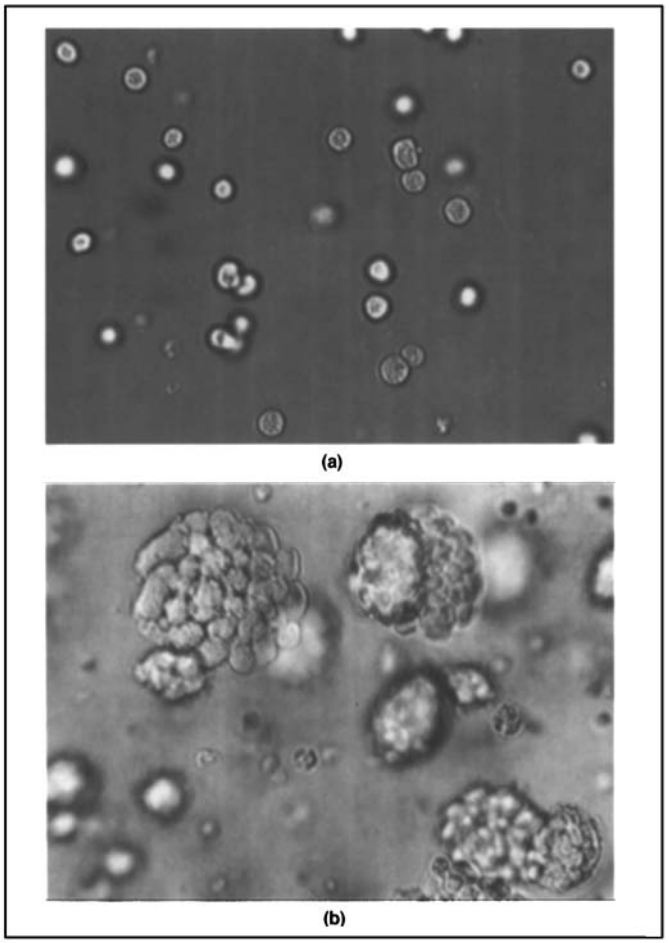

Figure 2. Hybridoma cells immobilized in a solidified agarose matrix.

(a) Immediately after immobilization, the cells are evenly distributed throughout the support. (b) As the cells proliferate, their positions become increasingly correlated and cell clusters develop. The CG7C7 hybridoma cell line was obtained from ATCC, and immobilization procedures are similar to those reported by Cadic et al. (1992).

control the placement of individual microstructural elements. Even for a relatively simple case of biological cells encapsulated in a gelatinous support material, a wide variety of structural characteristics can be considered, depending on (1) cell geometry (spheres, cylinders, ellipsoids, or more complex shapes); (2) cell sizes (identical or variable); (3) whether the cells are uniformly distributed or clustered (and if clustered, the cluster size distribution); and (4) whether the cells are isolated or in contact (and if they contact, to what extent they deform each other's boundaries). Clearly, some restrictions are necessary. Consistent with some types of mammalian cells, the simulated cells are round (in 2-D) or spherical (in 3-D) and have a uniform size. Cells are placed in a square (2-D) or cubic (3-D) region with periodic boundaries, so that if a cell intersects a boundary, it partially reappears on the opposite boundary. This procedure effectively simulates an infinitely large structure. The size of the placement region is large compared to the cells to avoid finite size effects. Cells are positioned one at a time until a desired area (2-D) or volume (3-D) fraction is achieved. The cell coordinates are generated using a random number generator and a specific set of placement rules, so that the entire structure is specified by the center coordinates and the diameter of the cells. Three types of structure have been investigated: uniformly placed nonoverlapping cells, cells clustered in groups of 50, and arbitrarily overlapping cells.

Nonoverlapping Cells. In experimental systems a short time after immobilization, encapsulated cells are evenly distributed throughout the support material (see Figure 2a). This situation is represented by placing nonoverlapping cells at positions determined by a random number generator in the placement region until the desired area or volume coverage is attained. New cells are checked for overlaps with previously placed cells, and overlapping cells are repositioned in a new location. The maximum cell fraction obtained without overlap is about 50% in two dimensions and about 45% in three dimensions. A typical simulated structure of nonoverlapping cells in two dimensions is illustrated in Figure 3a, while in three dimensions is depicted in Figure 4.

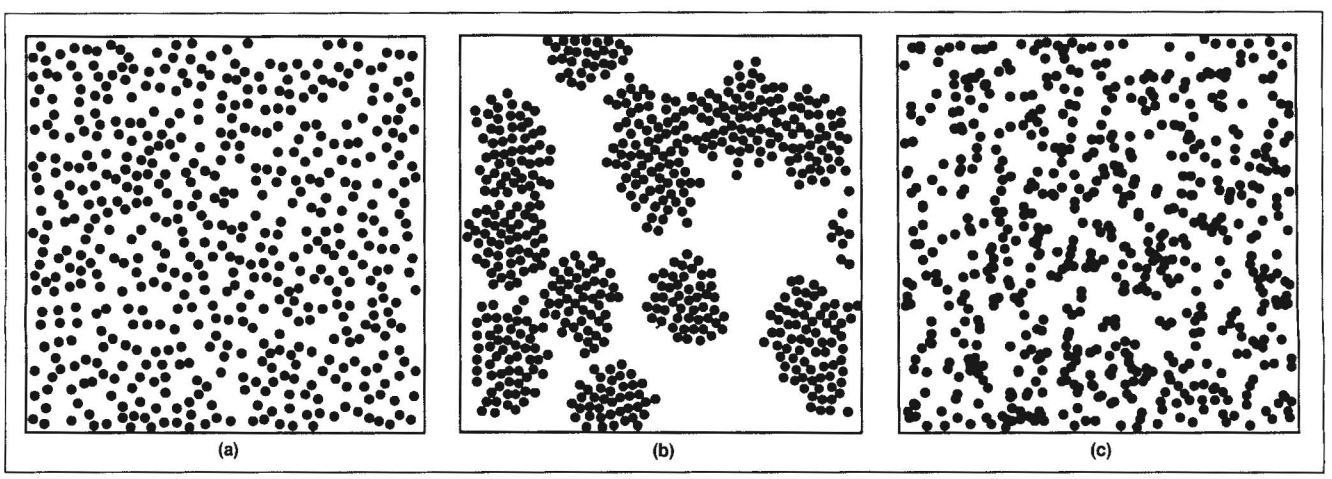

Figure 3. Computational representations of simulated cell structures in 2-D with a cell fraction of 0.30.

Cells with a diameter of 15 nodes were positioned (a) uniformly without overlap, (b) in nonoverlapping clusters of 50 cells, and (c) with arbitrarily overlapping positions.

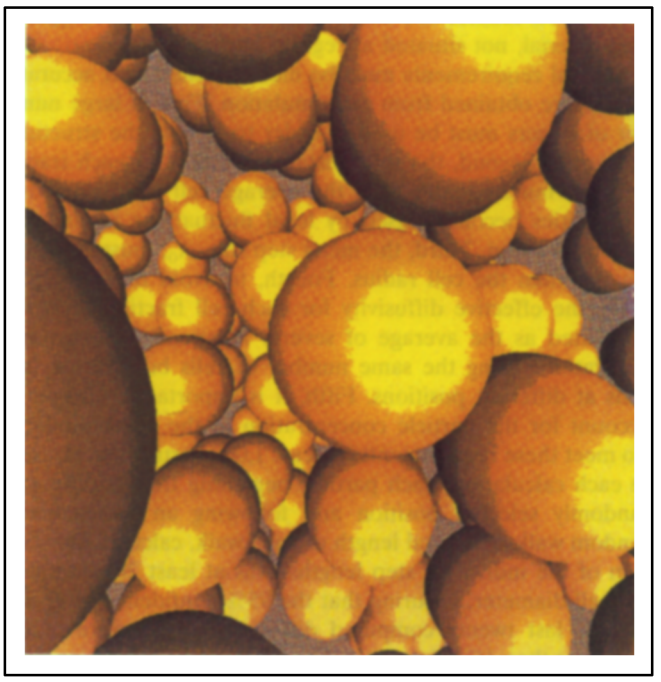

Figure 4. Simulated positioning of nonoverlapping spherical cells of identical size in three dimensions with a volume fraction of 0.30.

Clustered Cells. In experimental immobilized cell systems, as the cells proliferate in the support material, progeny remain in close proximity to the parent cells, leading to the development of highly compact cell clusters (see Figure 2b). Simulated cell clusters (Figure 3b) have been used here to assess the effect of cell proliferation and placement on the effective diffusivity of the molecules in the system. Cells are positioned in the support following placement rules that mimic the proliferation of immobilized cells into large clusters (see Figure 5). An initial seed cell is placed randomly in the support. A second cell is placed at a random angular position adjacent to the first cell so that the center coordinates are separated by a distance slightly larger than one cell diameter (the cells almost touch each other). A third cell is then placed at a random angle, next to the first cell. This new cell is not allowed to overlap with any existing cells; overlapping cells are rejected. A fourth cell is placed next to the second cell. A fifth cell is placed next to the first cell, a sixth cell is placed next to the second cell, a seventh next to the third, and so on. If no progeny can be placed next to a given cell without overlapping, this cell is labeled "contact-inhibited" and is ignored from then on. The cell clusters "grow" almost exclusively from the outer edge of the cluster once the interior cells have become surrounded by others. The placement procedure is repeated until the appropriate number of cells in the cluster has been obtained. Cell fractions are manipulated by changing the number of clusters while keeping the cell diameter and the cluster size constant. Clusters of 50 cells (in 2-D) produced by this method are generally round (see Figure 3b).

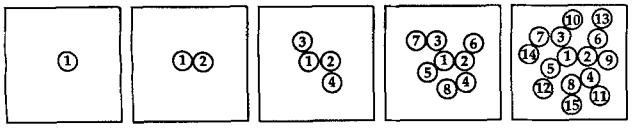

Figure 5. Placement of a cell cluster containing 15 cells.

The initial seed cell, ①, is placed at a random position in the support. All subsequent cells are placed directly next to the seed cell or next to progeny of the seed in the numerical order displayed here.

Overlapping Cells. When immobilized cells are in close contact, they slightly deform each other's boundaries, producing what appears to be a set of squashed spheres. This type of structure is computationally represented by randomly positioning cells in the placement region without regard to whether new cells overlap with previously existing cells (Figure 3c). This approach allows the attainment of cell fractions in the full range $0 \leq \phi \leq 1.0$. The cell fraction is accounted for by the true area fraction (in 2-D) of cell coverage; overlapping regions are counted only once, regardless of how many cells cover the area. The area fraction covered by cells follows from the Poisson relation:

$$\phi = 1 - \exp[-N\pi R^2/L^2], \tag{3}$$

where N is the number of cells, R is the radius of a cell, and L is the length of one edge of the placement domain (Avrami, 1940).

Diffusion simulation

The diffusivity of a molecule in a given structural representation is determined by monitoring the distance traveled by tracer particles undergoing a random walk through the structure in a given time. Tracers are initiated at random positions in the structure. Molecular diffusion outside the cells (that is, in the support material) is modeled as a series of steps in random directions with step length $\lambda = -\lambda_0 \log \epsilon$, where ϵ is a random number with uniform probability in the interval [0, 1] and λ_0 is the average step size. This step length distribution is extrapolated from the survival equation for particle collisions based on the kinetic theory of gases (Tabor, 1979). Particles inside a cell take steps with sizes $\lambda = -\gamma\lambda_0 \log \epsilon$, where $\gamma = D_c/D_0$ is a constant less than 1. A schematic particle trajectory in three dimensions is presented in Figure 6. The straight line displacement, X, that each particle travels in a given time is used to compute the mean-squared displacement, $\langle X^2 \rangle$, averaged for a large number of tracer particles. The effective diffusivity, D_{eff}, is computed using the Brownian motion relationship:

$$D_{\text{eff}} = \frac{\langle X^2 \rangle}{2d\Sigma\lambda}, \tag{4}$$

where $d = 2$ and 3 apply to 2-D and 3-D systems, respectively, and $\Sigma\lambda$ corresponds to the summation of the individual particle steps. This mean-displacement method has been selected over the first passage time approach (Kim and Torquato, 1991; Reyes and Iglesia, 1991a,b) based on ease of development and implementation.

Since the length of individual steps along the random walk depends on whether the tracer is inside a cell or in the support material, at each step one must know the tracer position

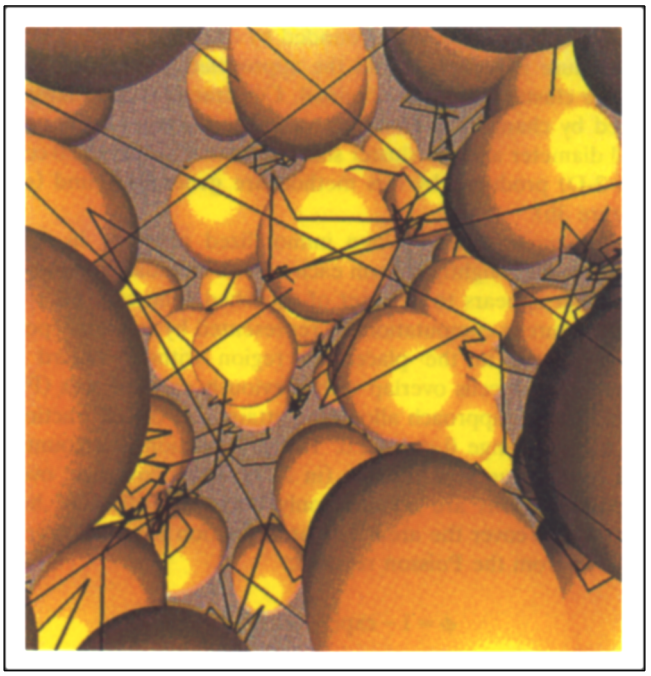

Figure 6. Representative trajectory of a tracer molecule diffusing through a 3-D structure of nonoverlapping, nonconductive cells ($D_0/D_c = \infty$).

relative to all the cells. To accomplish this, the placement domain is discretized into a logical array. A matrix of nodal points (1,000×1,000 in 2-D and 100×100×100 in 3-D) is overlaid across the system. Nodes of the array within one cell radius from the coordinates of a cell center are assigned a logical value ·TRUE·; remaining nodes are assigned ·FALSE·. The discretization procedure is similar to that used by Lee and Torquato (1988) to determine the porosity of two-phase disordered media. To determine whether a tracer is inside a cell or in the support, the algorithm simply recalls the value of the node nearest to the tracer; a returned value of ·TRUE· means that the tracer is inside a cell and the tracer diffusivity is equal to D_c. If the returned value is ·FALSE·, then the diffusivity equals D_0. This procedure is very efficient and can be readily implemented for arbitrarily shaped microstructures. Materials consisting of more than two phases could be represented by a straightforward extension of this method. An additional advantage of this method is that 2-D and 3-D simulations demand roughly similar amounts of computer time. This is rarely the case in computer simulations; typically, 3-D computations are much more time intensive than their 2-D counterparts. Drawbacks of this procedure are the large memory requirements of the nodal matrix, which limits the resolution of the placement domain, and the slight distortion of the cells imposed by the discretization procedure. Since the steps taken by the tracer particles are small compared to the cell diameter, and since a large number of nodes is used to represent each cell (a diameter of 15 nodes per cell yields a total of 177 nodes for a 2-D cell and 1,767 nodes for a 3-D cell), this distortion has little effect on the overall results. It is important to note that although cells are represented by a set of nodal points on a lattice, cell centers are distributed continuously throughout the material, not situated at regular lattice positions.

Several requirements must be met to ensure that accurate results are obtained from the simulation. First, a large number of tracers must be used in order to sample the structure uniformly. Second, the total distance traveled by each tracer must be much greater than the average cell size, otherwise diffusivities become biased by local fluctuations in the cell volume fraction. Third, the mean step size, λ_0, must be much smaller than the cell radius. Fourth, to avoid finite size effects, the effective diffusivity for each cell fraction must be computed as the average of several independent structural realizations using the same number of cells but placing the cells at different positions. Fifth, it is important to properly account for the particle concentration at the cell boundary. To meet these requirements, at least 1,000 particles were used in each calculation, each particle beginning from a different randomly selected position and following an independent random walk. The total length of each walk, calculated as the sum of the individual step lengths, was at least 20,000 times the cell diameter, ensuring that the 95% confidence intervals for the last twenty computed diffusivity values were much narrower than 1% of the calculated diffusivity, indicating that the tracers sampled a representative region of the structure. The mean step length, λ_0, was less than 0.035 times the cell diameter to minimize edge effects created by the jagged nodal representations of the cell boundaries. Two methods can be used to equilibrate the concentration on either face of the boundary. The first is to allow only a certain percentage of particles to cross into the other phase (Kim and Torquato, 1991). A second method, used in our simulation, is to allow all particles to cross, but to immediately change the particle step length to reflect the new particle environment. Finally, the effective diffusivity for each cell fraction was calculated as the average from ten different structural realizations. This ensured that the standard deviation between runs was less than 0.015.

Results and Discussion

Diffusivity predictions for uniformly distributed, nonoverlapping cells in two dimensions are presented in Figure 7. Simulation results are presented as normalized diffusivities, D_{eff}/D_0, where D_{eff} is the calculated effective diffusivity and D_0 is the diffusivity in the cell-free support. Four sets of results are shown in Figure 7, each corresponding to a different diffusivity ratio ($D_0/D_c = 2$, 3, 4, and 5) for cell area fractions up to 0.50. Diffusivity values are highly dependent on the cell fraction, particularly at low cell fractions; they decrease nonlinearly with increasing cell fraction, and are inversely related to the diffusivity ratio. Each set of results approaches the theoretical lower limit $D_{\text{eff}}/D_0 \rightarrow D_c/D_0$ at $\phi \rightarrow 1.0$. The effect of D_0/D_c becomes smaller at higher ratios, that is, the results at $D_0/D_c = 5$ are relatively close to those for $D_0/D_c = 4$, indicating that the simulation conditions are approaching the lower bound on the diffusivity ($D_c = 0$).

Figure 8 displays normalized diffusivity results for nonoverlapping cells uniformly distributed in three dimensions. Five diffusivity ratios ($D_0/D_c = 2$, 3, 4, 5, ∞) were investigated for cell fractions ranging from 0.0 to 0.45. Diffusivity values are again highly dependent on both the cell fraction and the dif-

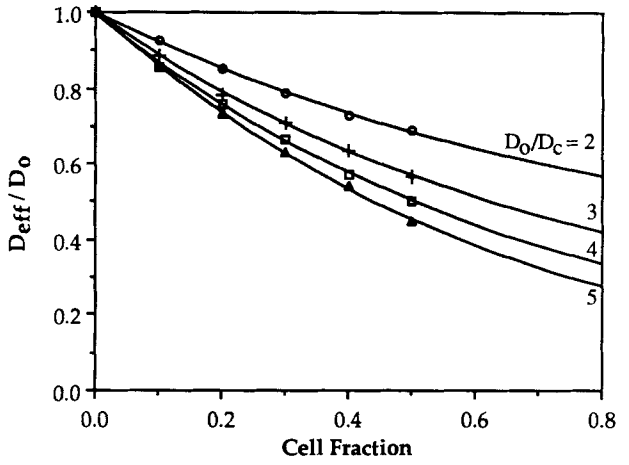

Figure 7. Monte Carlo diffusivity predictions for uniformly distributed, nonoverlapping cells in two dimensions for various diffusivity ratios and cell fractions.

Solid curves represent least-squares fits with third-order polynomials.

fusivity ratio. The diffusivity decreases with increasing cell fraction from the upper bound of $D_{eff} = D_0$ (at $\phi = 0.0$) to the theoretical lower bound of $D_{eff} \to D_c$ (at $\phi \to 1.0$). At a given cell fraction, the higher D_0/D_c, the lower the normalized diffusivity D_{eff}/D_0. At higher diffusivity ratios the effective diffusivity is more sensitive to small changes in the cell fraction than at lower diffusivity ratios. These follow similar trends observed in Figure 7; the diffusivity approaches a constant value with increasing diffusivity ratio.

To assess the validity of the simulations, diffusivity results were compared with results obtained from theoretical models. A polynomial fit to the 3-D simulation results (solid curves) are compared with predictions from Maxwell's model

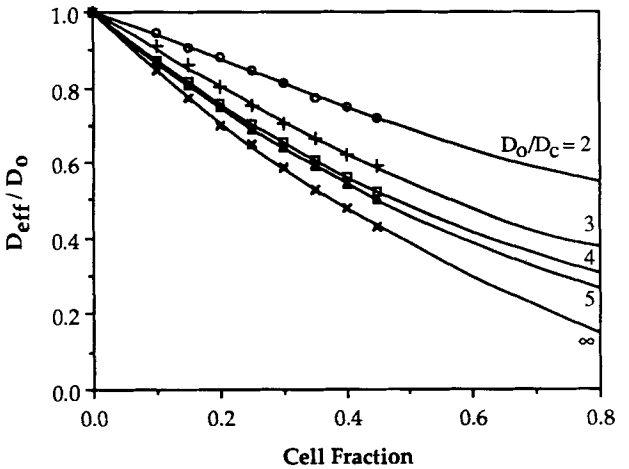

Figure 8. Diffusivity predictions for uniformly distributed, nonoverlapping cells in three dimensions for various diffusivity ratios and cell fractions.

Solid curves represent least-squares fits with third-order polynomials.

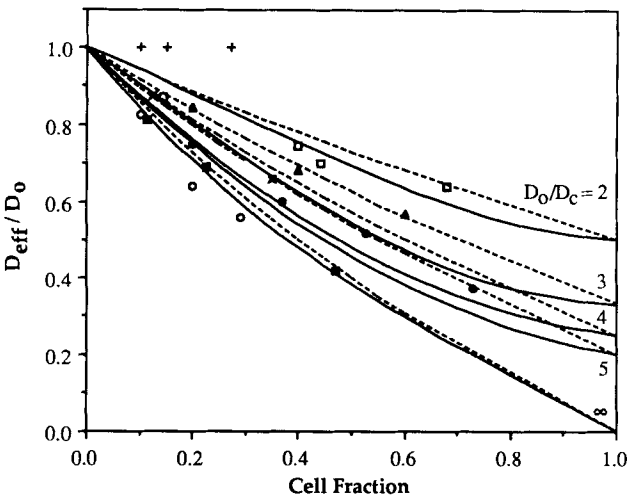

Figure 9. Comparison of predicted diffusivities (——), experimentally measured diffusivities (○, ●, □, ■, ▲, +, x), and Maxwell's model predictions (– – –).

The solid curves represent predictions at various diffusivity ratios and cell fractions in three dimensions (as in Figure 8). The experimental data are from: Axelsson and Persson (1988)—■; DeBacker et al. (1992)—x; Korgel et al. (1992)—○; Kurosawa et al. (1989)—+; Libicki et al. (1988)—●; Scott et al. (1989)—▲; and Sun et al. (1989)—□. Maxwell's model predictions have the same diffusivity ratios as those used in the simulations.

(1954) (dashed curves) in Figure 9. Both Maxwell's model and the simulations are based on similar assumptions about the material structure, and yield the same maximum and minimum diffusivity values at low ($\phi = 0.0$) and high ($\phi = 1.0$) cell fractions, but Maxwell's model yields a more linear approximation between these limits than do the simulations. For nonconductive inclusions ($D_0/D_c = \infty$) the simulation results are in very good agreement with Maxwell's model. With $D_0/D_c > 3$ Maxwell's model predicts much higher diffusivities than those generated by the simulations. The disagreement is likely due to the first-order approximation of Maxwell's model, which strictly applies to low-volume fractions of inclusions. In particular, this figure suggests that for $D_0/D_c = 3$ or higher, Maxwell's model generates poor predictions for inclusion fractions greater than 0.20. Simulation results fall within the Hashin and Shtrikman bounds (1962), slightly above the lower bound (not shown). The upper Hashin-Shtrikman bound is Maxwell's model, so the deviation between the simulation results and Maxwell's model is the maximum deviation permitted by the Hashin-Shtrikman bounds. The diffusivity predictions are also consistent with experimentally determined diffusivities in immobilized cell systems for a variety of diffusing species, cell types, and support materials reported by several investigators (symbols in Figure 9). For example, DeBacker et al. (1992) measured the diffusivity of glucose in an alginate gel containing cells, and their data correspond closely to the curve for $D_0/D_c = 3$.

The simulation results described so far apply to nonoverlapping, uniformly distributed cells. However, as mentioned earlier, as immobilized cells proliferate, they develop into highly compact cell clusters with highly correlated cell positions. For such cases, the assumption of random cell place-

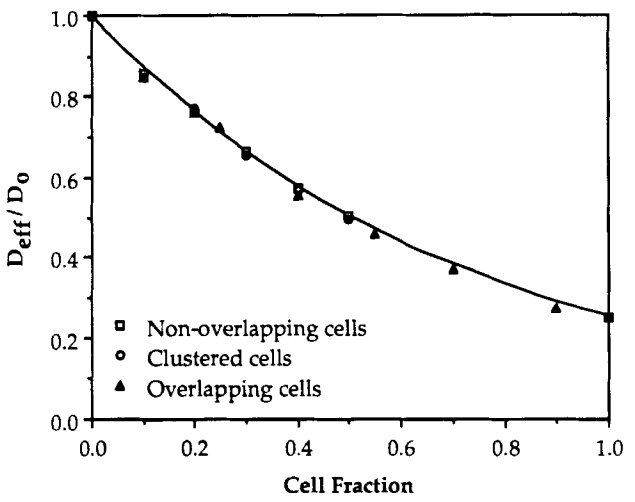

Figure 10. Comparison of diffusivities calculated in two dimensions for a system with $D_0/D_c = 4$.

Cells are uniformly distributed without overlap (□), clustered in groups of 50 (○), or allowed to arbitrarily overlap (△).

ment is no longer realistic (see Figure 2). To assess the effect of cell clustering on the effective diffusivity, simulations were conducted in two dimensions with cells placed in clusters of 50. Results with $D_0/D_c = 4$ are compared with those for uniformly distributed (nonclustered) cells with $D_0/D_c = 4$ (Figure 10). Due to the uneven spatial distribution of cells, the clustered system has regions with high and low local diffusivity. However, the results show that the overall effective diffusivity of a system with clustered cells is essentially the same as that with uniformly distributed cells; the only influential parameters appear to be once again the cell fraction and the diffusivity ratio. Simulations were also conducted with a system consisting of arbitrarily overlapping cells. The computed diffusivity for a range of cell fractions up to $\phi = 1.00$ for overlapping cells is essentially the same as that in both the uniformly distributed nonoverlapping and the clustered nonoverlapping systems (Figure 10). The results for overlapping cells are in very good agreement with the Devera and Strieder bounds (1977) for overlapping spheres of arbitrary D_0/D_c (comparison is not shown). Simulation results for overlapping cells are close (within 1 percent, on the "safe" side) to the lower bound for all points except $\phi = 0.1$, which deviates from the lower bound by approximately 4%. The largest statistical errors (maximum standard deviation) arise at the lowest volume fractions, because structures are composed of only a few cells, and under such conditions many structural realizations are necessary to obtain good statistical accuracy. Fortunately, for low-volume fractions, theoretical models are highly accurate. As the volume fraction increases, the standard deviation for different structural realizations decreases, making simulations the most accurate alternative.

When the diffusivity of a solute in the immobilized cell system is calculated as a macroscopic (long-distance) effective diffusivity, the spatial distribution of the cells does not appear to have a major influence on the results for the conditions evaluated here. This is in qualitative agreement with the recent results of El-Kareh et al. (1993), who investigated idealized cell configurations consisting of periodic arrays of rectangular cells to represent highly compact cellular tissue. Normalized diffusivities were calculated for varying interstitial volume fractions $(1 - \phi)$, where antibodies diffuse only in the region between cells. The shape and spatial arrangement of the cells had little effect on the diffusivity of antibodies in tissue. These results deviate from those obtained by several researchers (Evans et al., 1980; Nakano and Evans, 1983; Reyes and Iglesia, 1991a; Kim and Torquato, 1992a,b) who reported that the material structure does play an important role in the diffusive properties of a multiphase system. However, these investigations were conducted with dramatically different solute diffusivities in the phases, and in some situations, one of the phases did not allow solute transport. Also, these investigations focused on the Knudsen diffusion and transition diffusion so that the diffusing species free path was not infinitely small compared with the structural material. In the multiconductive ($D_0/D_c \ll \infty$) biological system studied here, the diffusivities in the two phases are moderately different from each other; there is no excluded volume in the material, and the structure seems to have no major effect on molecular diffusion.

Conclusions and Future Work

The decrease in the effective diffusivity of cellular nutrients with increasing cell fraction can limit the supply of nutrients and hence affect the growth and maintenance of cells in an immobilized cell system. Accurate assessment of the diffusivities is therefore important in bioengineering applications. Methods for generating model multiphase materials that capture key morphological features of immobilized cell systems are described in this article. The simulated structures consist of uniformly distributed, clustered, and overlapping cells positioned in a conductive support material. A Monte Carlo algorithm was developed to calculate effective diffusivities in such materials for a wide range of cell fractions and diffusivity ratios. Diffusivities depend strongly on the cell fraction and the diffusivity ratio; high cell fractions and large diffusivity ratios lead to low effective diffusivities. Predictions agree with reported experimental values and are consistent with the models of Maxwell (1954), Hashin and Shtrikman (1962), and Devera and Strieder (1977).

The results described in this article have focused on biological applications, but are valid in general for heterogeneous materials consisting of multiple spherical inclusions with diffusivities different from that of the continuous phase. The 2-D diffusivity results, for example, can be applied to diffusion of small molecules within a membrane (see, for example, Saxton, 1993; Qian et al., 1993). Likewise, the 3-D diffusivity results can be used to describe diffusion through polymer blends where the less permeable phase has been broken into drops. The Monte Carlo algorithm can be modified to study systems of increasing morphological complexity. Our current efforts in this area address the extension of the simulation technique to incorporate chemical reactions in the cells and the addition of membrane resistances to diffusion.

Acknowledgments

This work was supported by grants from the Exxon Foundation and the Merck Foundation to F.J.M., and by a grant from the New

Jersey Center for Biomaterials and Medical Devices to H.M.B. M.R.R. gratefully acknowledges Exxon Research and Engineering Company for supporting a stimulating summer internship.

Notation

$D_0/D_c = 1/\gamma$ = diffusitivity ratio
D_{eff}/D_0 = normalized effective diffusivity
X = straight-line particle displacement

Greek letters

λ_c = mean step size in the cellular phase

Literature Cited

Abbasi, M. H., J. W. Evans, and I. S. Abramson, "Diffusion of Gases in Porous Solids: Monte Carlo Simulations in the Knudsen and Ordinary Diffusion Regimes," *AIChE J.*, **29**, 617 (1983).

Akanni, K. A., and J. W. Evans, "Effective Transport Coefficients in Heterogeneous Media," *Chem. Eng. Sci.*, **42**, 1945 (1987).

Avrami, M., "Kinetics of Phase Change: II. Transformation-Time Relations for Random Distribution of Nuclei," *J. Chem. Phys.*, **8**, 212 (1940).

Axelsson, A., and B. Persson, "Determination of Effective Diffusion Coefficients in Calcium Alginate Gel Plates with Varying Yeast Cell Content," *Appl. Bio. Biotech.*, **18**, 231 (1988).

Boyer, P. M., and J. T. Hsu, "Experimental Studies of Restricted Protein Diffusion in an Agarose Matrix," *AIChE J.*, **38**, 259 (1992).

Cadic, C., B. Dupuy, I. Pianet, M. Merle, C. Margerin, and J. H. Bezian, "*In Vitro* Culture of Hybridoma Cells in Agarose Beads Producing Antibody Secretion for-Two Weeks," *Biotech. Bioeng.*, **39**, 108 (1992).

Chiew, Y. C., and E. D. Glandt, "The Effect of Structure on the Conductivity of a Dispersion," *J. Coll. Inter. Sci.*, **94**, 90 (1983).

Chiew, Y. C., "Effective Conductivity of Two-Phase Materials Consisting of Long Parallel Cylinders," *J. Appl. Phys.*, **67**, 1684 (1990).

Cukier, R. I., S. Y. Sheu, and J. Tobochnik, "Random-Walk Simulation of the Dielectric Constant of a Composite Material," *Phys. Rev. B*, **42**, 5342 (1990).

DeBacker, L., S. Devleminck, R. Willaert, and G. Baron, "Reaction and Diffusion in a Gel Membrane Reactor Containing Immobilized Cells," *Biotech. Bioeng.*, **40**, 322 (1992).

DeVera, A. L., and W. Strieder, "Upper and Lower Bounds on the Thermal Conductivity of a Random, Two-Phase Material," *J. Phys. Chem.*, **81**, 1783 (1977).

El-Kareh, A. W., S. L. Braunstein, and T. W. Secomb, "Effect of Cell Arrangement and Interstitial Volume Fraction on the Diffusivity of Monoclonal Antibody in Tissue," *Biophys. J.*, **64**, 1638 (1993).

Evans, J. W., M. H. Abbasi, and A. Sarin, "A Monte Carlo Simulation of the Diffusion of Gases in Porous Solids," *J. Chem. Phys.*, **72**, 2967 (1980).

Franko, A. J., and R. M. Sutherland, "Oxygen Diffusion Distance and Development of Necrosis in Multicell Spheroids," *Rad. Res.*, **79**, 439 (1979).

Freyer, J. P., and R. M. Sutherland, "Determination of Diffusion Constants for Metabolites in Multicell Tumor Spheroids," *Oxygen Transport to Tissue*, Vol. IV, H. I. Bicker, and D. F. Bruley, eds., Plenum, New York, p. 463 (1981).

Hannoun, B. J. M., and G. Stephanopoulos, "Diffusion Coefficients of Glucose and Ethanol in Cell-free and Cell-occupied Calcium Alginate Membranes," *Biotech. Bioeng.*, **28**, 829 (1986).

Hashin, Z., and S. Shtrikman, "A Variational Approach to the Theory of the Effective Magnetic Permeability of Multiphase Materials," *J. Appl. Phys.*, **33**, 3125 (1962).

Itamunoala, G. F., "Limitations of Methods of Determining Effective Diffusive Coefficients in Cell Immobilization Matrices," *Biotech. Bioeng.*, **31**, 714 (1988).

Kao, H. P., J. R. Abney, and A. S. Verkman, "Determinants of the Translational Mobility of a Small Solute in Cell Cyroplasm," *J. Cell. Bio.*, **120**, 175 (1993).

Karel, S. F., S. B. Libicki, and C. R. Robertson, "The Immobilization of Whole Cells: Engineering Principles," *Chem. Eng. Sci.*, **40**, 1321 (1985).

Karel, S. F., and C. R. Robertson, "Autoradiographic Determination of Mass-Transfer Limitations in Immobilized Cell Reactors," *Biotech. Bioeng.*, **34**, 320 (1989).

Kawashiro, T., W. Nusse, and P. Scheid, "Determination of Diffusivity of Oxygen and Carbon Dioxide in Respiring Tissue: Results in Rat Skeletal Muscle," *Pflugers Arch.*, **359**, 231 (1975).

Kim, I. C., and S. Torquato, "Determination of the Effective Conductivity of Heterogenous Media by Brownian Motion Simulation," *J. Appl. Phys.*, **68**, 3892 (1990).

Kim, I. C., and S. Torquato, "First-Passage-Time Calculation of the Conductivity of Continuum Models of Multiphase Composites," *Phys. Rev. A*, **43**, 3198 (1991).

Kim, I. C., and S. Torquato, "Effective Conductivity of Suspension of Overlapping Spheres," *J. Appl. Phys.*, **71**, 2727 (1992a).

Kim, I. C., and S. Torquato, "Diffusion of Finite-Sized Brownian Particles in Porous Media," *J. Chem. Phys.*, **96**, 1498 (1992b).

Korgel, B. A., A. Rotem, and H. G. Monbouquette, "Effective Diffusivity of Galactose in Calcium Alginate Gels Containing Immobilized *Zymomonas mobilis*," *Biotechnol. Prog.*, **8**, 111 (1992).

Kurosawa, H., M. Matsumura, and H. Tanaka, "Oxygen Diffusivity in Gel Beads Containing Viable Cells," *Biotech. Bioeng.*, **34**, 926 (1989).

Lazar, A., "Immobilization of Animal Cells in Fixed Bed Bioreactors," *Biotech. Adv.*, **9**, 411 (1991).

Lee, G. M., and B. O. Palsson, "Immobilization Can Improve the Stability of Hybridoma Antibody Productivity in Serum-Free Media," *Biotech. Bioeng.*, **36**, 1049 (1990).

Lee, G. M., and B. O. Palsson, "Stability of Antibody Productivity Is Improved When Hybridoma Cells are Entrapped in Calcium Alginate Beads," *Biotech. Bioeng.*, **42**, 1131 (1993).

Lee, S. B., and S. Torquato, "Porosity for the Penetrable-Concentric-Shell Model of Two-Phase Disordered Media: Computer Simulation Results," *J. Chem. Phys.*, **89**, 3258 (1988).

Libicki, S. B., P. M. Salmon, and C. R. Robertson, "The Effective Diffusive Permeability of a Nonreacting Solute in Microbial Cell Aggregates," *Biotech. Bioeng.*, **32**, 68 (1988).

Luby-Phelps, K., P. E. Castle, D. L., Taylor, and F. Lanni, "Hindered Diffusion of Inert Tracer Particles in the Cytoplasm of Mouse 3T3 Cells," *PNAS*, **84**, 4910 (1987).

Martinsen, A., G. Skjak-Braek, and O. Smidsrod, "Alginate as Immobilization Material: I. Correlation between Chemical and Physical Properties of Alginate Gel Beads," *Biotech. Bioeng.*, **33**, 79 (1989).

Maxwell, J. C., *A Treatise on Electricity and Magnetism*, 3rd ed., Vol. 1, Dover, New York (1954).

Nakano, Y., and J. W. Evans, "Monte Carlo Simulation of Diffusion of Gases in a Porous Solid: Calculations for a New Class of Solids," *J. Chem. Phys.*, **78**, 2568 (1983).

Pu, H., and R. Yang, "Diffusion of Sucrose and Yohimbine in Calcium Alginate Gel Beads with or without Entrapped Plant Cells," *Biotech. Bioeng.*, **32**, 891 (1988).

Qian, H., M. P. Sheetz, and E. L. Elson, "Single Particle Tracking—Analysis of Diffusion and Flow in Two-Dimensional Systems," *Biophys. J.*, **60**, 910 (1993).

Reyes, S. C., and E. Iglesia, "Effective Diffusivities in Catalyst Pellets: New Model Porous Structures and Transport Simulation Techniques," *J. Cat.*, **129**, 457 (1991a).

Reyes, S. C., and E. Iglesia, "Monte Carlo Simulations of Structural Properties of Packed Beds," *Chem. Eng. Sci.*, **46**, 1089 (1991b).

Saxton, M. J., "Lateral Diffusion in an Archipelago—Single-Particle Diffusion," *Biophys. J.*, **64**, 1766 (1993).

Scott, C. D., C. A. Woodward, and J. E. Thompson, "Solute Diffusion in Biocatalyst Gel Beads Containing Biocatalysis and other Additives," *Enzyme Micro. Tech.*, **11**, 258 (1989).

Sun, Y., S. Furusaki, A. Yamauchi, and K. Ichimura, "Diffusivity of Oxygen into Carriers Entrapping Whole Cells," *Biotech. Bioeng.*, **34**, 55 (1989).

Tabor, D., *Gases, Liquids, and Solids*, 2nd ed., Cambridge Univ. Press, Cambridge, England, p. 84 (1979).
Tanaka, H., M. Matsumura, and I. A. Veliky, "Diffusion Characteristics of Substrates in Ca-Alginate Gel Beads," *Biotech. Bioeng.*, **26**, 53 (1984).
Tobochnik, J., D. Laing, and G. Wilson, "Random-Walk Calculation of Conductivity in Continuum Percolation," *Phys. Rev. A*, **41**, 3052 (1990).
Torquato, S., "Diffusion and Reaction Among Traps: Some Theoretical and Simulation Results," *J. Stat. Phys.*, **65**, 1173 (1991).
Torquato, S., and M. Avellaneda, "Diffusion and Reaction in Heterogeneous Media: Pore Size Distribution, Relaxation Times, and Mean Survival Time," *J. Chem. Phys.*, **95**, 6477 (1991).
Wakao, N., and J. M. Smith, "Diffusion in Catalyst Pellets," *Chem. Eng. Sci.*, **17**, 825 (1962).
Wakao, N., and J. M. Smith, "Diffusion and Reaction in Porous Catalyst," *Ind. Eng. Chem. Fund.*, **3**, 123 (1964).
Westrin, B. A., and A. Axelsson, "Diffusion in Gels Containing Immobilized Cells: A Critical Review," *Biotech. Bioeng.*, **38**, 439 (1991).
Zheng, L. H., and Y. C. Chiew, "Computer Simulation of Diffusion-Controlled Reactions in Dispersions of Spherical Sinks," *J. Chem. Phys.*, **90**, 322 (1989).

Manuscript received Nov. 29, 1993, and revision received May 16, 1994.